The Ag-InP(110) interface: Photoemission studies of interfacial reactions and Schottky-barrier formation

I. A. Babalola,* W. G. Petro, T. Kendelewicz,† I. Lindau, and W. E. Spicer
Stanford Electronics Laboratories, Stanford University, Stanford, California 94305
(Received 29 August 1983; revised manuscript received 19 March 1984)

The effects of interfacial reaction at Ag-InP(110) interfaces have been studied with soft-x-ray photoemission spectroscopy of the core levels and valence band. By systematically increasing the Ag coverages, we have been able to identify two coverage ranges with different stages of physical interactions and interface developments from a detailed study of the In $4d$, P $2p$, and Ag $3d$ core levels as well as valence-band structures. At lower Ag coverages [$0<\Theta<1$ monolayer (ML)], identified as the "band-bending region," both the In $4d$ and P $2p$ levels shift by the same amount with no measurable changes in the core-level shapes for both n and p type, and a continuous and monotonic shift of the Ag $3d$ core levels toward their metallic positions is observed with increased Ag coverages. At high coverages ($1\leq\Theta<72$ ML), identified as the "intermixed region," the presence of P atoms at the topmost layer and evidence of dissociated In were observed from the core-level variations and relative intensity studies at the interface. In both regions, island growth of the overlayer is observed. The surface-Fermi-level (E_{Fs}) pinning position, determined from core-level movements in this region, can be affected by the intermixing of Ag with dissolved InP constituents. Ag interacts with InP in a way that is essentially different in details as compared with other metals, to the extent that the model identifying Ag as a nonreactive metal on InP may need to be modified.

I. INTRODUCTION

The InP-metal interface has received attention recently in an attempt to understand the basic physical process responsible for Schottky-barrier formation at metal-(III-V compound) interfaces in general.[1–4] Many experimental techniques—electrical measurements[5–7] (I-V and C-V), structure and photoemission,[8–11] and combinations of these—have been used in new attempts to focus attention on the interactions taking place between the metal overlayer and the semiconductor. These interactions have been considered in a few cases[7] as the main determining factor for the observed surface-Fermi-level (E_{Fs}) pinning at the interface. However, the detailed processes of the interactions are yet to be clearly understood. One of the conclusions of some of these studies[6,7] is the classification of the InP-metal interface into reactive and nonreactive categories, based on the variations in InP-metal interface behavior for different metals with their heats of reaction, characterized by the index of behavior, S.[12,13] On the basis of these studies and bulk thermodynamic data, some metal overlayers have also been classified as reactive and others as nonreactive.[5,6,13] Although it has been shown that S is not a meaningful parameter,[5,14] since local chemical effects could play a more critical part, other justifications are needed to support the classification of the metal-semiconductor interface into reactive and nonreactive categories. In the work presented here, both a conventional helium light source and monochromatic soft x rays from the Stanford Synchrotron Radiation Laboratory (SSRL) were used to systematically study the Ag-InP interface from submonolayer coverages up to "thick" coverages. In our detailed work, we followed the E_{Fs} movement at the interface (by gradually increasing the Ag coverage) as a means of measuring the Schottky-barrier heights. We followed the changes in interface properties using relative intensity profiles and detailed studies of the In $4d$, P $2p$, and Ag $3d$ core levels and valence-band structures as a function of Ag coverage. These enable us to address the question of abruptness of the Ag/InP interface and to study the nature of the interaction between metal overlayer and semiconductor substrate. We shall show that Ag reacts in a way different in detail when compared with observations on other "nonreactive" metals. The analysis presented here on the Ag/InP(110) interface is expected to form the basis of a detailed comparative study for other metal-(III-V compound) interfaces.

This paper will be presented in the following way: The experimental method will be presented in Sec. II. The details of our results for (1) the low-Ag-coverage interval and (2) the high-Ag-coverage interval will be presented and discussed in Sec. III. Here we shall present under Sec. III A the details of interactions at the interface for the two coverage intervals, and in Sec. III B we shall discuss the Schottky-barrier measurements. In the conclusion, we shall summarize our results on the effects of the observed interaction and the way it relates to the Schottky-barrier measurement at the Ag/InP(110) interface.

II. EXPERIMENTAL

Clean surfaces of the InP(110) crystal were prepared by cleaving *in situ* in ultrahigh vacuum at a base pressure of 6×10^{-11} Torr. The InP single-crystal samples used in the experiments were n type with carrier concentration $n=6\times10^{17}$ cm^{-3} and p type with $p=3\times10^{18}$ cm^{-3} sup-

plied by MCP Electronics. During the preliminary experiments with the He lamp as a light source, we studied two cleaves of each type and similarly with the synchrotron radiation.

The Ag overlayers were prepared by evaporation from a bead on a molybdenum wire and the thickness was monitored and controlled by using two quartz-crystal monitors. The first monitor was placed very close to the evaporation source (on the evaporator flange), while the second one was on the sample manipulator so that it could be placed in the sample position. The first monitor was initially calibrated against the second one, and the geometrical correction factor was determined. Exposures were carried out by opening the evaporator shutter to the sample for a few ($\simeq$10) seconds, and the sample was positioned about 10 cm away from the evaporator to reduce heating of the sample surface. The evaporation rate was continuously monitored by means of the first thickness monitor, especially for higher coverages. By this method the error in the determination of Ag coverages is less than 20% at low coverages [$\Theta < 1$ monolayer (ML)] and less than 10% for the higher coverages. Ag coverages were determined from the amount of Ag incident on the sample surface, and we assume here a unity sticking coefficient so that 1 ML represents one Ag atom per surface (indium and phosphorus) atom, i.e., 1 ML$=8.2\times10^{14}$ cm^{-2}. The maximum pressure during the evaporation was 1×10^{-10} Torr at the higher coverages. This good pressure was achieved by a thorough initial outgassing of the metal source.

The photoemission energy distribution curves (EDC's) were taken with a double-pass cylindrical mirror analyzer (CMA). Valence-band spectra were measured at 21.2 eV and In $4d$ core lines monitored at 40.8 eV on the helium light source. The synchrotron-radiation source used was one of the 4° beam lines (I-1) at SSRL, employing a grazing incidence monochromator which provided an intense polarized monochromatic[15] beam in the range from 65 to 600 eV. In these experiments the photon count rate was typically about 10^4 counts/sec. This provided the high statistics in the data recorded here. The resolution of the monochromator is typically $\sim$0.2 Å,[15] while that of the CMA used here is between 0.15 and 0.3 eV.[16] The accuracy of relative core-level shifts is about $\pm$0.05 eV and the absolute location of core-level energies is accurate to within $\pm$0.1 eV.

The unique property, the tunability of the synchrotron radiation, has been of much advantage in these experiments. The escape depth of electrons recorded here has been determined[16] to be within the range from 5 to 10 Å. This means that the spectra taken in these experiments have maximum surface sensitivity. For instance, the valence bands and indium core levels were each taken at photon energies of 80 and 120 eV where the escape depths are 5–6 Å. Details of the experimental methods used to determine E_{Fs} have been discussed elsewhere and will not be repeated here.[1,17]

III. RESULTS AND DISCUSSION

The soft-x-ray photoemission spectroscopy (SXPS) results (taken at SSRL) are summarized in representative plots. Figures 1(a)–1(d) and 2 show the coverage dependence of In $4d$ and P $2p$ core levels taken at respective photon energies of $h\nu=80$ and 185 eV for n and p types. We monitored the Ag $3d$ core levels at $h\nu=425$ eV as shown in Fig. 3 for p-type InP(110). In Figs. 4(a) and (b), we show the coverage dependence of the valence-band spectra taken at $h\nu=120$ eV. In Fig. 5 we present the physical information deduced from the Ag $4d$ core levels as a function of coverage, while in Figs. 6(a) and 6(b) we present the relative intensity profiles of the core levels monitored in these experiments.

We shall divide the discussion of these results into two Ag coverage intervals. This is done because the two intervals correspond to different stages in the physical interaction and interface developments. This division is not distinct but is based on observed different features which will become clearer later. These intervals are (1) the band-bending region ($0<\Theta<1$ ML) and (2) the intermixing region ($1<\Theta<72$ ML).

A. Interaction at the Ag-InP(110) interface

1. *Band-bending region ($\Theta<1$ ML)*

From the monitored peaks (A and B) of Ag $4d$ in the valence band we could follow the development of the Ag $4d$ with increasing Ag coverages. There is the gradual increase of the two peaks and, in addition, the gradual increase in the energy separation (ΔE) of the two prominent peaks with Ag coverages, as shown on the valence-band spectra in Fig. 4(a) for lower Ag coverages and Fig. 4(b) for high coverages. A summary of the variation of ΔE with Θ is shown in Fig. 5. The exponential increase of ΔE is faster at the lower Ag coverages, increasing slowly toward 1.35 eV at 72 ML coverage. The behavior of Ag $4d$ seen here is very similar to that observed for Au $5d$ for the Au/InP system where ΔE tends toward the value of metallic Au.[9] This has been observed also on many metal/semiconductor interfaces[18,19] and, in particular, on Si (Refs. 20 and 21) where the shift of only one peak of Ag $4d$ towards lower binding energies (E_B) was observed due to the limit of their resolution; the total shift of $\sim$0.3 eV measured in the Ag-Si experiment is close to average of the two shifts observed here—$\sim$0.2 eV for peak A and $\sim$0.5 eV for peak B in Fig. 4(b). We also monitored the Ag $3d$ core levels, and we observed that the monitored peaks moved toward lower binding energies. As seen in Fig. 3, this shift is over and above band bending, which has stabilized for all coverages equal to and above 0.79 ML. We found that the separation of these two peaks due to spin-orbit splitting is independent of Θ.

We conclude that the Ag photoemission peaks are atomiclike at lower coverages, as shown by ΔE for the Ag $4d$ being close to the atomic value, but move toward a bandlike situation with increased Θ. Additional evidence of this is the shift of the Ag $3d$ toward lower binding energies, saturating at about 25 ML when it is close to the binding energy of metallic Ag $3d$. At this coverage, we can observe a well-defined metallic Fermi edge in the valence-band spectra of $h\nu=120$ eV shown in Fig. 4(b). The behavior of Ag will be discussed here with that of In $4d$ and P $2p$.

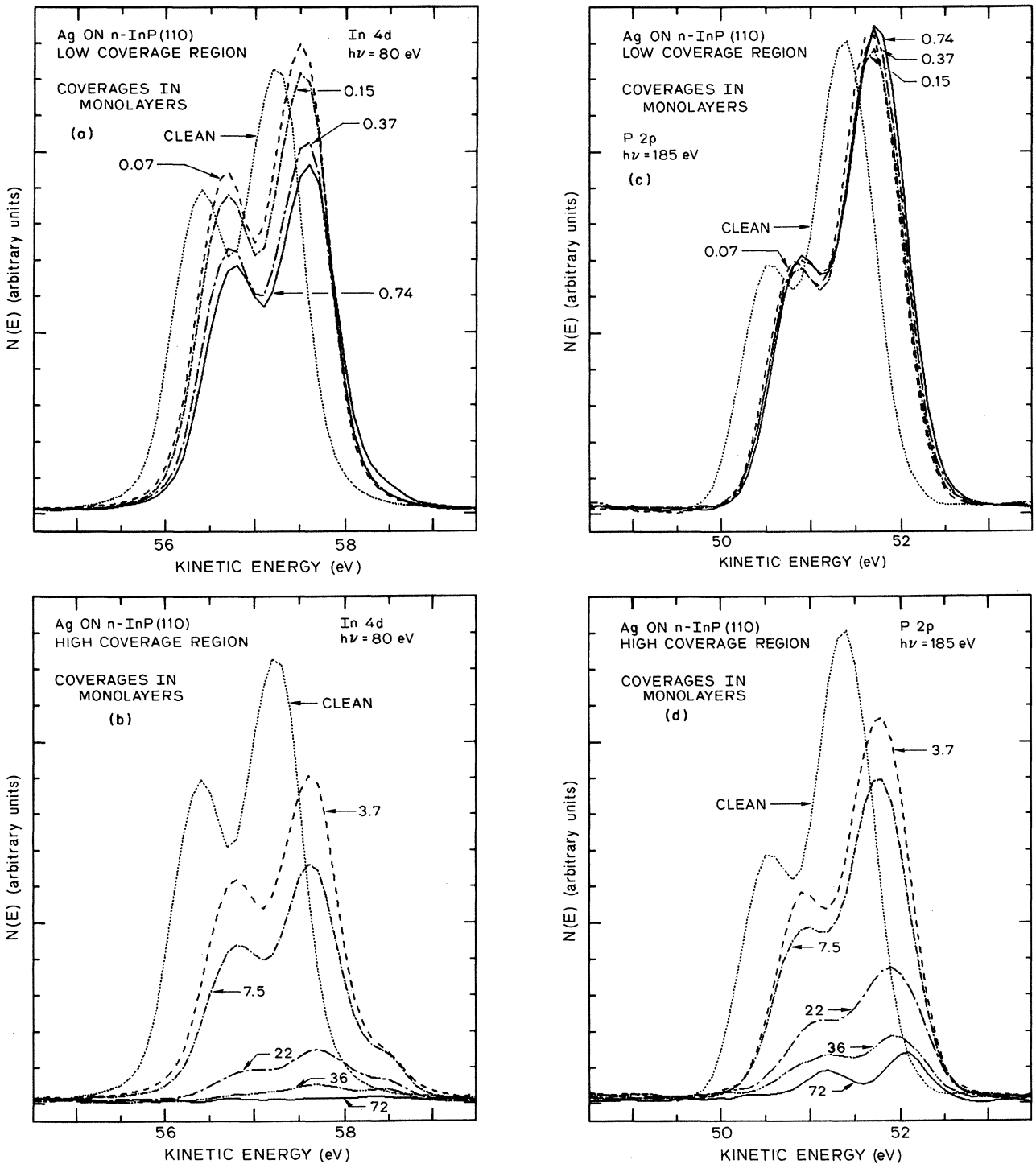

FIG. 1. (a) In 4*d* core-level spectra at a photon energy of 80 eV as a function of Ag coverage on *n*-type InP(110) for the low Ag coverage interval. (b) In 4*d* core-level spectra at a photon energy of 80 eV as a function of Ag coverage on *n*-type InP(110) for the high Ag coverage interval. (c) P 2*p* core-level spectra taken at a photon energy of 185 eV as a function of Ag coverage on *n*-type InP for the low Ag coverage interval. (d) P 2*p* core-level spectra taken at a photon energy of 185 eV as a function of Ag coverage on *n*-type InP(110) for the high Ag coverage interval.

(i) In 4*d* core levels are shown in Figs. 1(a) and 1(b) for *n*-type InP and in Fig. 2 for *p*-type InP. We observed that there is no measurable change in the shape of the structures up to 0.79 ML.

(ii) P 2*p* core levels shown in Figs. 1(c) and 1(d) for *n* type and in Fig. 2 for *p* type did not change shape within the lower coverage interval of $0 < \Theta < 0.79$ ML.

(iii) Both the In 4*d* and P 2*p* core levels shift towards

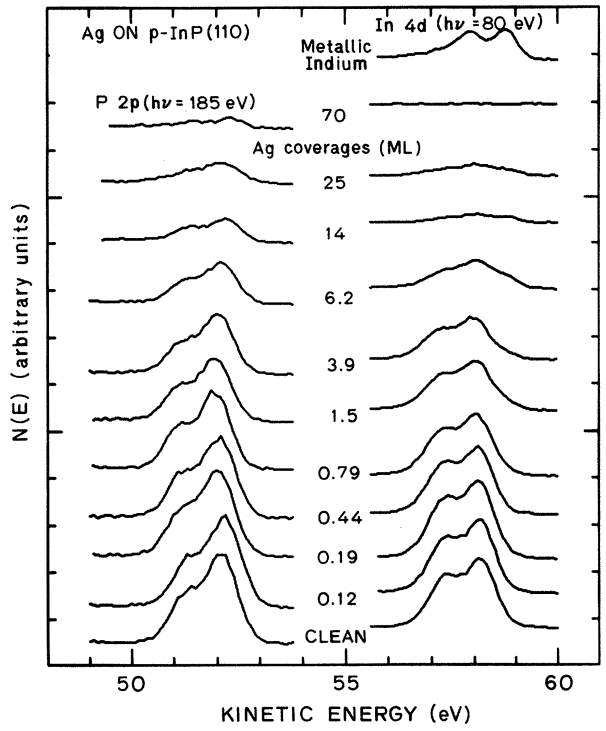

FIG. 2. P $2p$ core levels taken at $h\nu = 185$ eV and In $4d$ core levels taken at $h\nu = 80$ eV as a function of Ag coverage on p-type InP(110).

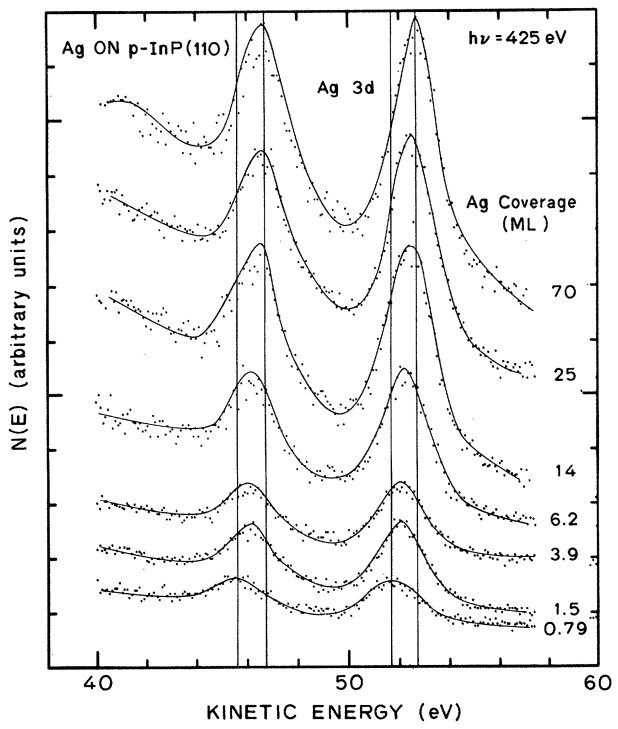

FIG. 3. Ag $3d$ core-level spectra taken at a photon energy of 425 eV as a function of Ag coverage on p-type InP(110). The lines show the total shift of the $3d$ peaks at the highest coverages with respect to those at 0.79 ML coverage.

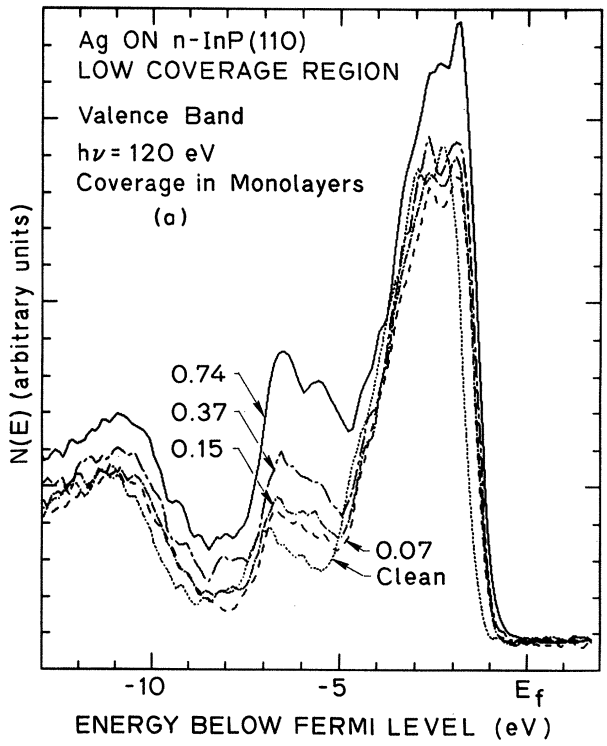

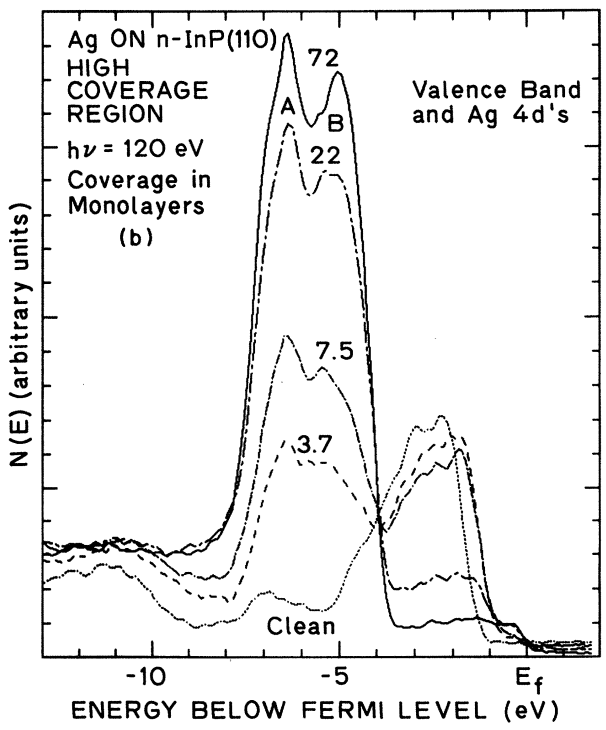

FIG. 4. (a) EDC's of the valence band taken at a photon energy of 120 eV as a function of Ag coverage on n-type InP(110) for the low coverage interval. (b) EDC's of the valence band taken at a photon energy of 120 eV as a function of Ag coverage on n-type InP(110) for the high coverage interval. The growth of Ag $4d$ is shown and marked A and B.

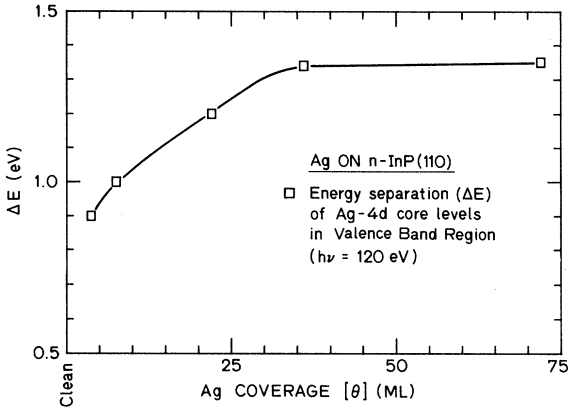

FIG. 5. Plot of the energy splitting (ΔE) of the two Ag $4d$ peaks A and B in the valence band taken at $h\nu=120$ eV as a function of Ag coverage Θ in ML.

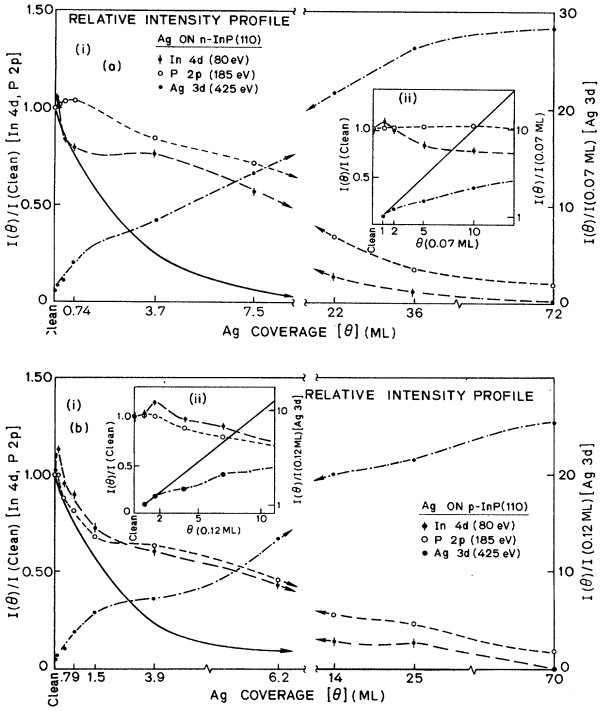

FIG. 6. (a) (i) Relative intensity profiles—$I(\Theta)/I$(clean) for In $4d$ and P $2p$ and $I(\Theta)/I$(0.07 ML), axis on the right, for Ag $3d$—as a function of average Ag coverage Θ in ML for n-type InP(110). The solid curve represents the exponential decay of the In $4d$ and P $2p$ expected for uniform growth of an abrupt Ag overlayer. (ii) Inset of intensity profiles for the band-bending region plotted as a function of Ag coverage in units 0.07 ML. The scale on the right-hand side (Ag $3d$) has been expanded relative to the scale on the left-hand side (In $4d$ and P $2p$). The solid line represents the Ag $3d$ increase expected for uniform growth of the Ag overlayer. (b) (i) Relative intensity profiles—$I(\Theta)/I$(clean) for In $4d$ and P $2p$ and $I(\Theta)/I$(0.12 ML), axis on the right-hand side, for Ag $3d$—as a function of average Ag coverage Θ in ML for p-type InP(110). The solid curve represents the exponential decay of the In $4d$ and P $2p$ expected for uniform growth of an abrupt Ag overlayer. (ii) Inset of intensity profiles for the band-bending region plotted as a function of Ag coverage in units of 0.12 ML. The scale on the right-hand side (Ag $3d$) has been expanded relative to the scale on the left-hand side (In $4d$ and P $2p$). The solid line represents the Ag $3d$ increase expected for uniform growth of the Ag overlayer.

lower binding energies on n type. The P $2p$ shift for p type is initially toward lower binding energy but beyond $\Theta=0.12$ ML gradually toward higher E_B. The In $4d$ shift for p type is initially toward higher E_B and thereafter relatively stable at the same final value as for the P $2p$.

(iv) Relative intensity profiles of In $4d$ and P $2p$ normalized to the intensities on clean InP, $I(\Theta)/I$(clean), are shown in Figs. 6(a) (i) and 6(b) (i). There is a large divergence between the results shown and the expected theoretical fall in intensity with Θ, and this will be discussed in the next section.

(v) Relative intensity profiles of the Ag $3d$ core level relative to the intensity for the first Ag deposition—$I(\Theta)/I$(0.07 ML) for n type and $I(\Theta)/I$(0.12 ML) for p type—are shown in the insets Figs. 6(a) (ii) and 6(b) (ii), respectively, for submonolayer Ag depositions. The increase in intensity is seen to be much slower than expected for uniform overgrowth of the first monolayer. This suggests the presence of three-dimensional island formation before the first monolayer is complete—in contrast to the Stranski-Krastanov growth mode.[22] This is discussed in more detail in the next section.

We can conclude on the basis of these observations that no clear evidence of interaction between the Ag and InP surface atoms can be observed in this coverage interval.

2. *Intermixing region ($1 \leq \Theta < 72$ ML)*

Within this high coverage interval the following experimental observations will guide the development of a model (or models) for the Ag/InP interface and the growth mechanism of Ag on InP.

(i) Splitting of the Ag $4d$ as shown in Fig. 5 has reached a plateau at about 36 ML with $\Delta E=1.35$ eV. The valence-band spectra in Fig. 4(b) show a metallic Fermi edge with the valence-band structure of InP completely covered by the Ag $4d$ structures.

(ii) Ag $3d$ core level continues to shift toward lower binding energy as shown in Fig. 3, reaching $E_B \approx 368$ eV relative to the Fermi level at $\Theta=72$ ML. However, the relative intensities $I(\Theta)/I$(0.1 ML) for both n and p types in Figs. 6(a) and 6(b) show a slow increase from about 0.74 to 3.9 ML followed by a faster increase then leveling off near 72 ML. The slow growth of the intensity of Ag $3d$ between 0.74 and 3.9 ML could support possible indiffusion of some silver atoms into InP as well as increasing island thickness.

(ii) In $4d$ and P $2p$ relative intensity profiles shown in Figs. 6(a) (i) and 6(b) (i) deviate very much from the expected exponential decay of the two core levels with Ag coverage. The rate of attenuation of the two peaks seen here is slower than expected. The solid curve shows the exponential decay of the In $4d$ and P $2p$ core-level intensi-

ties expected for uniform growth of an abrupt Ag overlayer, and is given by

$$I(\Theta)/I(\text{clean})=\exp[-t\Theta/L(E)\cos\phi]\ ,$$

where Θ is in ML, $t=1.4$ Å is the thickness of 1 ML of Ag as determined by the bulk Ag density, $L(E)=5$ Å is the scattering length in Ag for electrons of ≈ 50 eV kinetic energy, and $\phi=42.6°$ is the angle between sample normal and emitted electron direction to CMA. By 72 ML, no In $4d$ could be seen; however, up to $\approx 10\%$ of the P $2p$ peak could be seen. We note the similarity in the pattern of attenuation of the two peaks, with In $4d$ falling faster than P $2p$.

(iv) Structures of the P $2p$ in Figs. 1(d) and 2 clearly show the slow attenuation of the peak identified in (iii) above. However, there is little noticeable change in the shape of these peaks up to 72 ML. The spin-orbit-split peaks are still identifiable even at the highest Ag coverage, with the measured half width close to that on clean InP for both n and p types.

(v) In $4d$ core-level structure changes dramatically beyond 0.79 ML as shown in Fig. 1(b) for n type and Fig. 2 for p type. An additional peak starts to develop on the lower-binding-energy side. The amplitude of this peak did not follow the same attenuation as the two spin-orbit-split peaks with increased Θ. The appearance of this new peak broadens the In $4d$ peak, and becomes very prominent at 22-ML Ag coverage when the heights of all In $4d$ peaks become compatible. In Fig. 7, we show our model of what is happening. Curve A is the In $4d$ core level monitored in this experiment for the clean p-type InP(110) surface, while B is the In $4d$ core level of metallic indium taken by evaporating a thick layer (≈ 200 Å) of In *in situ* onto a stainless-steel substrate and monitored at the same photon energy ($h\nu=80$ eV) as in the Ag-InP experiment. Each of these curves has been shifted along the kinetic energy axis and scaled along the intensity axis so that their sum (dashed curve) matches as closely as possible the actual curve obtained for 6.2 ML of Ag on p-type InP(110) (dotted curve). The similarity of the two curves is remarkable. From this deconvolution process, we observe that the recorded In $4d$ at this coverage is the summation of In from the InP substrate and dissociated metalliclike In.

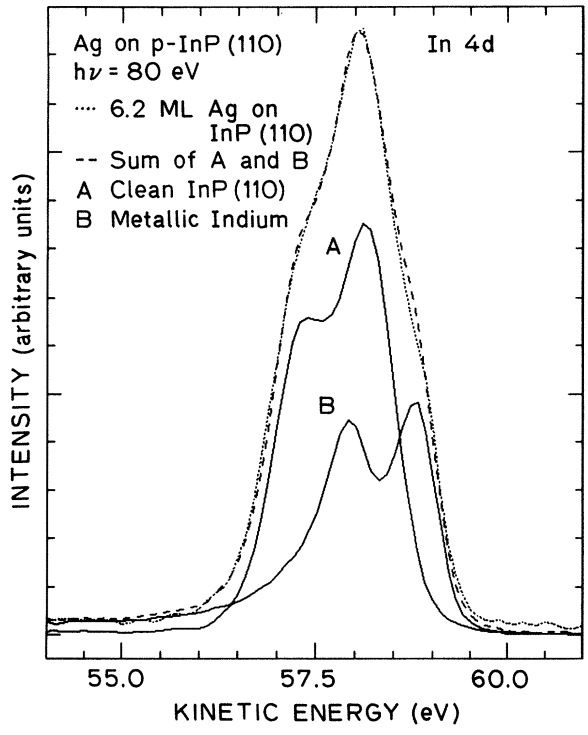

FIG. 7. Deconvolution of the In $4d$ core level for p-type InP(110) taken at 6.2 ML Ag coverage (dotted curve). The dashed curve is the sum of curves A and B.

Our observations from the above-listed experimental facts are that Ag interacts with the InP surface atoms in such a way as to dissolve the surface atoms at these coverages. At coverages between 3.7 and 36 ML we were monitoring a combination of In $4d$ from the substrate and dissociated indium. The fact that we could monitor the P $2p$ at the highest coverage of 72 ML when no In $4d$ signal could be seen is an indication that we were monitoring P on (or within) the topmost layer of Ag. This picture becomes more reasonable when we consider the fact that the Ag thickness of ≈ 100 Å is over an order of magnitude greater than the electron escape depths at these photon energies.

The close trends in the variation of relative intensities of In $4d$ and P $2p$ and the fact that they deviate from the expected exponential decay shown here could support the island-growth mechanism of Stranski-Krastanov as seen in the case of Ag on Si.[21,22] However, as shown in the insets of Figs. 6(a) and 6(b), the Ag $3d$ intensity increases much more slowly than the linear increase which would be expected for uniform growth of the first monolayer. This suggests that Ag island formation occurs even for submonolayer coverages. Islanding at higher coverages is indicated in the In $4d$ spectra at 22 and 36 ML of Ag coverage shown in Fig. 1(b). In both cases there is a strong substrate component which would not be present if the entire surface were uniformly covered by Ag films of the corresponding thicknesses. The large P-to-In ratio, particularly at the higher coverages, indicates intermixing of the Ag with the substrate and segregation of P at the topmost surface layer. Here we have been able to address the question of the average depth distribution of Ag and the intermixing of In and P atoms on the basis of the relative intensities and core-level structural studies. To go beyond here on the growth mechanism of Ag on InP and details of the interaction between Ag and InP surface atoms will require an additional detailed structural study using low-energy electron diffraction (LEED) and other diffraction and depth-profiling techniques as useful supplements to the photoemission results discussed here.

There have been few published works on the Ag-(III-V compound) interface reaction and, in particular, on the Ag/InP interface. This may be due to the accepted view that Ag behaves in an identical way with Au on most III-V compounds. Williams *et al.* in their series of studies of metals on III-V compounds have used both a C-V electrical method[5,6] and SXPS techniques[8] to study the Ag/InP(110) interface and the problem of intermixing at

the interface. They stressed that the nature of the chemical composition of the outermost atomic layer on the Ag/InP(110) surface has a drastic influence on the contact behavior. McKinley *et al.*[23] have reached conclusions very similar to ours using different techniques. They see evidence of island formation based on LEED, Auger-intensity profiles, and angle-resolved ultraviolet photoemission spectroscopy, and evidence of intermixing based on Auger depth profiles and adhesion measurements. Others[7] have used SXPS in addition to electrical methods to study the Ag/InP interface in combination with other metals and have suggested on the basis of their SXPS results and bulk thermodynamic data the presence of intermixing and interdiffusion at the interface. However, some of the data used lacked the level of spectral resolution and detailed study for one metal as presented in this work. Farrow and co-workers[11,24] in their study of the Ag/InP(001) interface observed epitaxial growth of Ag islands. We have also observed evidence of islanding for Ag on InP(110) as discussed previously. However, Farrow *et al.* found no evidence for any interfacial reaction or alloying from TEM studies and observed a low ($\approx$0.1-eV) barrier height, both of which differ from what we observe for Ag on the cleaved (110) surface. These differences may be accounted for by the different crystal face used (001) and/or the different method of preparation of the clean surface (argon-ion bombardment followed by annealing to 250–300 °C), which results in excess surface In islands and may also cause surface and subsurface lattice damage.[11] An abrupt interface has also been observed for Ag/GaAs(110) (Refs. 25 and 26), consistent with the trend that metal/GaAs(110) interfaces are less reactive than the corresponding metal/InP(110) interfaces as observed for Au (Refs. 9 and 27) and Al.[28]

B. Schottky-barrier height measurement

Core-level movement observed in photoemission experiments has been used as a method of determining surface-Fermi-level movement[1,18,29] because the binding energy of a core level in a semiconductor does not change with band bending when determined relative to the valence-band maximum at the surface. However, in cases where dissociation of the surface atoms of the substrate semiconductor occurs to the extent that free metallic atoms at the surface are observed, then the above method of determining E_{Fs} movement may not be accurate. From our discussion in the early section, the above situation holds for the high coverage interval which we have identified as the intermixed region. This situation also appears to hold true, though to a lesser extent, for the Au/GaAs(110) interface[1,18,27,29] at room temperature. We shall differentiate between the two coverage intervals in our discussion of the Fermi-level movement at the interface.

1. *Band-bending region ($0<\Theta<1$ ML)*

We have shown from the detailed study of the In 4*d*, P 2*p*, and Ag 3*d* core levels the Ag 4*d* structures in the valence band, and the respective core-level relative intensity profiles that no observable changes in the structure of the substrate surface atoms as a result of serious atomic disruption could be detected. However, there is an initial shift of $\sim$0.27 eV for both In 4*d* and P 2*p* core levels after the initial Ag deposition of $\sim$0.07 ML on *n* type. The shift gradually increased with Ag coverage to 0.35 eV at 0.74 ML coverage, as shown in Fig. 1(a) for In 4*d* and 1(c) for P 2*p*, and as summarized in Fig. 8. On *p* type, E_{Fs} was pinned at about 0.4 eV from the valence-band maximum (VBM) on the clean surface. The initial coverage of 0.12 ML caused the P 2*p* core level to shift toward lower binding energy (which implies movement of E_{Fs} toward the VBM), while the In 4*d* moved toward slightly higher binding energy. Then the P 2*p* core level shifted toward higher binding energy and the In 4*d* remained almost unchanged with Θ until both attained a total shift of about $\sim$0.50 eV at 0.44 ML. The details of these movements are shown in Fig. 2 and summarized in Fig. 8. These core-level shifts measured within this interval are considered to be due to band bending, resulting in a total Schottky-barrier height of $\sim$0.5 eV. This is because observations of the core-level structures and intensities do not support any atomic dissociation from the InP surface.

2. *Intermixed region ($\Theta \geq 1$ ML)*

From Figs. 1(d) and 2, we find that the P 2*p* core levels continued to shift toward lower binding energy on both *n* and *p* type, and, if we interpret this to be the Fermi-level movement at the interface, it implies that E_{Fs} continued to drop toward the VBM. However, this example is much different than when we refer to the details of interactions observed from (a) the dramatic changes in the structure of the In 4*d* core level, and (b) the fact that we are now observing free P in the topmost layer of Ag. The movement of the core level recorded within this interval cannot be identified as E_{Fs} movement at the interface. This is because the shifts measured here are for P in the Ag layer and dissociated In. We consider that much of the core-level shifts measured in this interval will be due to chemical shifts arising from the interaction of Ag with the InP surface atoms, and the presence of In and P atoms in a different environment with Ag atoms as neighbors.

If we sum up the total barrier height measured as equal to 0.4 eV on *n* type,[30] our result is in close agreement with the measurement of 0.47 eV by the *C-V* electrical method and 0.42 eV by the *I-V* method for Ag deposited on atom-

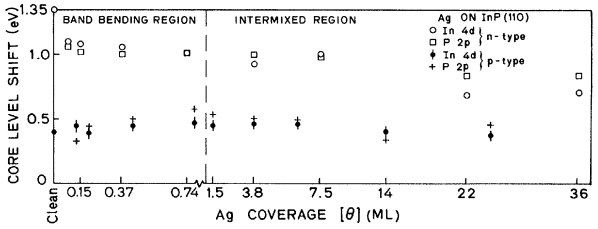

FIG. 8. In 4*d* and P 2*p* core-level shifts plotted as a function of Ag coverage for both *n*- and *p*-type InP(110). The quantity plotted along the vertical axis is given by E_{Fs}(clean) $-E_{\mathrm{VBM}}$(clean) $-[E_{k,\text{In 4d or P 2p}}(\Theta) - E_{k,\text{In 4d or P 2p}}(\text{clean})]$ for both *n* and *p* types.

ically clean InP(110) carried out by Williams and coworkers.[5,8]

From this study and similar work on Au-InP(110) (Ref. 9) it is clear that each metal reacts with the surface atoms in a unique and different way, and a clear understanding of the reactions taking place is essential to the understanding of the mechanism responsible for the Fermi-level movement. From this work it is also clear that it is not adequate in the case of InP(110) to follow the movement of core levels of one component and identify this as Fermi-level movement at the interface. This can only be correct when there are no clear evidences of intermixing, resulting from interaction of the metal with the substrate atom, as presented here. The concept which classified metals into reactive and nonreactive categories appears to be an oversimplification of a complex problem of the different ways each metal reacts with the substrate InP surface atoms. On the other hand, our results and analysis presented here show that ranges of Fermi-level pinning positions, determined from core-level shifts for different metals, may not be the correct way of showing the dependence of Schottky-barrier heights on chemical bonding and diffusion, resulting from the different ways the metals react with the InP surface atoms in the high coverage interval. We would also like to observe that a clear understanding of the way each metal interacts with the host substrate surface atoms may be basic to the understanding of Schottky-barrier formation with a combination of metals on III-V compounds.

The present result of Schottky-barrier measurement can be explained on the basis of the unified defect model applied to metals on InP(110) which has received extensive reports and discussion in the literature, and will therefore not be repeated here.[1,2,8,9,31–33] The interface defect level responsible for E_{Fs} pinning on InP has been located at 0.9 ± 0.1 eV above the VBM (Refs. 8, 31, and 33), and this has been associated with acceptor levels originating from missing indium.[8,31] However, Dow and Allen[4] have suggested that the defect responsible for this pinning is an antisite defect, not a cation vacancy. Their calculations also suggest that the In vacancy may account for the observed pinning of the clean cleaved p-type surface at 0.4—0.5 eV above the VBM. This pinning position has been observed in other work[2] and was attributed to an extrinsic defect. These locations of the interface defect levels are in agreement with the measurement of the Schottky barrier height in this work. The thermodynamic processes involved in the case of Ag on InP(110) fit into the general picture for metal III-V semiconductor compounds, which has been discussed in detail in earlier work.[1,2,31,33] The possibility of Ag cluster formation leading to defect formation as suggested by Zunger[34] for Al may also play a role, particularly for the n-type sample. On the p-type sample the pinning was dominated by defects present on the cleaved surface and remained essentially unchanged for subsequent Ag deposition.

Ludeke *et al.*[26] have presented a model based on interface states directly associated with the pure metal clusters. This model is most appropriate for systems which have negligible adsorbate-substrate interaction and which exhibit the continuous variation in Fermi-level position for both n and p type for coverages from $\sim10^{-2}$ to 10 ML as observed by Ludeke *et al.*[26] for Ag/GaAs(110). However, the stronger metal-substrate interaction for Ag/InP(110) makes such a model less applicable, and the fact that the Fermi level is stable from $\simeq0.1$ to 10 ML (Ref. 30) suggests that the states associated with Ag clusters of increasing size are not the dominant effect in this case. The model also cannot be used to account for the pinning observed on the clean cleaved p-type surface when no Ag is present. One other model—which has been proposed to explain the E_{Fs} pinning for a large number of metal/(III-V compound) interfaces—is the effective work-function model of Freeouf and Woodall,[35] in which the Schottky-barrier height is determined by the work-function difference between the semiconductor and clusters of anion-rich material at the interface. The simplest application of this model (using a phosphorous work function of 5.0 eV) gives barrier heights which differ significantly from our observed values for both n and p type. Indeed, our observation of P outdiffusion argues against the presence of anion clusters at the interface. More sophisticated applications of the model (possibly using the work function of Ag) may give better results on n type, but it is difficult to see how to apply the model to the observed complex situation of an unknown distribution of Ag islands with intermixed P and dissociated In. Additional discussion of the applicability of the effective work-function model to a number of systems is given in Ref. 36.

IV. CONCLUSIONS

A systematic photoemission investigation of the Ag/InP(110) interface, using to our advantage the tunability of the synchrotron radiation for optimum surface sensitivity, shows that at lower Ag coverages ($\Theta<1$ ML) there is no measurable evidence of early interaction of Ag with the InP surface atoms. We observed shifts of both In $4d$ and P $2p$ by the same amount and in the same direction on n type and equal total shifts on p type. This region has therefore been identified as the band-bending region, and the total core-level shift of ~0.4 eV has been regarded as Fermi-level movement since there are no evidences of significant dissolving of the InP surface atoms. However, we present evidence of dissociation of In atoms and accumulation of P in the topmost layer of Ag for high coverages ($1\leq\Theta<72$ ML). On account of the evidence of unique interactions observed in this interval (from the details of core-level studies), we have identified this region as the intermixed region and a high percentage of the core-level shifts measured here have been regarded as chemical shifts; therefore, ranges of E_{Fs} pinning positions based on core-level shifts in this intermixed region require separation of band-bending and chemical effects.[30] These studies have shown the unique way in which Ag reacts with the InP(110) surface which is different in many ways from that of Au (Ref. 9), Cu (Ref. 37), and Al.[28] Therefore, the classification of metal overlayers into reactive and nonreactive categories may be an oversimplification for the case of metals on InP(110). On the

method of separation of E_{Fs} movement from chemical shifts in the intermixed region, other experimental techniques (e.g., I-V measurements) in addition to photoemission will be useful. Additional work using techniques such as LEED and Auger depth profiling will give further information on the rate of intermixing and the thickness of the intermixed region. Furthermore, detailed study of the Ag/InP(110) interface at different temperatures would give additional information on the models proposed for the growth of Ag films on InP(110) (in the high coverage interval) and also on the amount of Ag diffusion into the InP bulk.

ACKNOWLEDGMENTS

We wish to acknowledge the assistance of J. A. Silberman in performing these experiments. This work was supported by the U.S. Defense Advanced Research Projects Agency and the U.S. Office of Naval Research under Contract No. N00014-83-K-0073 and the Solar Energy Research Institute under Subcontract No. XW-1-1181-1. The experiments were performed at the Stanford Synchrotron Radiation Laboratory which is supported by the U.S. Department of Energy (Office of Basic Energy Sciences) and by the National Science Foundation (Division of Materials Research).

---

*Permanent address: Department of Physics, University of Ibadan, Ibadan, Nigeria.

†On leave from the Institute of Physics, Polish Academy of Sciences, Warsaw, Poland.

[1]I. Lindau, P. W. Chye, C. M. Garner, P. Pianetta, C. Y. Su, and W. E. Spicer, J. Vac. Sci. Technol. 15, 1332 (1978); P. Chye, I. Lindau, P. Pianetta, C. M. Garner, C. Y. Su, and W. E. Spicer, Phys. Rev. B 18, 5545 (1978).

[2]W. E. Spicer, P. W. Chye, P. R. Skeath, C. Y. Su, and I. Lindau, J. Vac. Sci. Technol. 16, 1422 (1979).

[3]M. S. Daw, D. L. Smith, C. A. Swarts, and T. C. McGill, J. Vac. Sci. Technol. 19, 508 (1981).

[4]J. D. Dow and R. E. Allen, J. Vac. Sci. Technol. 20, 659 (1982).

[5]R. H. Williams, R. R. Varma, and A. McKinley, J. Phys. C 10, 4545 (1977).

[6]R. H. Williams, V. Montgomery, and R. R. Varma, J. Phys. C 11, L735 (1978).

[7]L. J. Brillson, C. F. Brucker, A. D. Katnani, N. G. Stoffel, and G. Margaritondo, J. Vac. Sci. Technol. 19, 661 (1981); 21, 564 (1982).

[8]R. H. Williams, A. McKinley, G. J. Hughes, V. Montgomery, and I. T. McGovern, J. Vac. Sci. Technol. 21, 594 (1982).

[9]I. A. Babalola, W. G. Petro, T. Kendelewicz, I. Lindau, and W. E. Spicer J. Vac. Sci. Technol. A 1, 762 (1983).

[10]A. Hiraki, S. Kim, W. Kammura, and M. Iwami, Surf. Sci. 86, 706 (1979).

[11]R. F. C. Farrow, A. G. Cullis, A. J. Grant, and J. E. Pattison, J. Cryst. Growth 45, 292 (1978).

[12]S. Kurtin, T. C. McGill, and C. A. Mead, Phys. Rev. Lett. 22, 1433 (1970).

[13]L. J. Brillson, Phys. Rev. Lett. 40, 260 (1978); J. Vac. Technol. 15, 1378 (1978).

[14]M. Schluter, Phys. Rev. B 17, 5044 (1978).

[15]F. C. Brown, R. Z. Bachrach, and N. Lien, Nucl. Instrum. Methods 152, 73 (1978).

[16]P. Pianetta, I. Lindau, and W. E. Spicer, in *Quantitative Surface Analysis of Materials,* ASTM STP 643, edited by N. S. McIntyre (American Society for Testing and Materials, Philadelphia, 1978), p. 105.

[17]P. Pianetta, I. Lindau, C. M. Garner, and W. E. Spicer, Phys. Rev. B 18, 2792 (1978).

[18]W. G. Petro, I. A. Babalola, P. Skeath, C. Y. Su, I. Hino, I. Lindau, and W. E. Spicer, J. Vac. Sci. Technol. 21, 585 (1982).

[19]L. Braicovich, C. M. Garner, P. R. Skeath, C. Y. Su, P. W. Chye, I. Lindau, and W. E. Spicer, Phys. Rev. B 20, 5121 (1976).

[20]G. Rossi, I. Abbati, I. Lindau, and W. E. Spicer, Appl. Surf. Sci. 9, 243 (1981).

[21]G. Rossi, I. Abbati, L. Braicovich, I. Lindau, and W. E. Spicer, Phys. Rev. B 25, 3619 (1982).

[22]J. A. Venables, J. Derrien, and A. P. Janssen, Surf. Sci. 95, 411 (1980).

[23]A. McKinley, A. W. Parke, and R. H. Williams, J. Phys. C 13, 6723 (1980).

[24]A. G. Cullis and R. F. C. Farrow, Thin Solid Films 58, 197 (1979).

[25]D. Bolmont, P. Chen, F. Proix, and C. A. Sebenne, J. Phys. C 15, 3639 (1982).

[26]R. Ludeke, T.-C. Chiang, and T. Miller, J. Vac. Sci. Technol. B 1, 581 (1983).

[27]W. G. Petro, I. A. Babalola, T. Kendelewicz, I. Lindau, and W. E. Spicer, J. Vac. Sci. Technol. A 1, 1181 (1983).

[28]T. Kendelewicz, W. G. Petro, I. A. Babalola, J. A. Silberman, I. Lindau, and W. E. Spicer, J. Vac. Technol. B 1, 623 (1983).

[29]P. Skeath, C. Y. Su, I. Hino, I. Lindau, and W. E. Spicer, Appl. Phys. Lett. 29, 349 (1981).

[30]W. G. Petro, T. Kendelewicz, I. A Babalola, I. Lindau, and W. E. Spicer, Mat. Res. Soc. Symp. Proc. (in press).

[31]R. H. Williams, R. R. Varma, and V. Montgomery, J. Vac. Sci. Technol. 16, 1418 (1979).

[32]P. R. Skeath, I. Lindau, P. W. Chye, C. Y. Su, and W. E. Spicer, J. Vac. Sci. Technol. 16, 1143 (1979).

[33]W. E. Spicer, S. Eglash, I. Lindau, C. Y. Su, and P. R. Skeath, Thin Solid Films 89, 447 (1982).

[34]A. Zunger, Phys. Rev. B 24, 4372 (1981).

[35]J. L. Freeouf and J. M. Woodall, Appl. Phys. Lett. 39, 727 (1981).

[36]R. H. Williams, Phys. Scr. T 1, 33 (1982).

[37]T. Kendelewicz, G. Rossi, W. G. Petro, I. A. Babalola, I. Lindau, and W. E. Spicer, J. Vac. Sci. Technol. B 1, 564 (1983).